



Yearly Energy, Exergy, and Environmental (3E) Analyses of A Photovoltaic Thermal Module and Solar Thermal Collector in Series

Sameer Teref Azeez Al-Aridhee*

Mohammad Moghiman**

*, **Department of Mechanical Engineering/ Ferdowsi University of Mashhad/
Mashhad/ Iran

**Email: eng.sameer3@gmail.com

***Email: moghiman@um.ac.ir

(Received 25 November 2022; Accepted 29 January 2023)

<https://doi.org/10.22153/kej.2023.01.001>

Abstract

The annual performance of a hybrid system of a flat plate photovoltaic thermal system and a solar thermal collector (PVT/ST) is numerically analyzed from the energy, exergy, and environmental (CO₂ reduction) viewpoints. This system can produce electricity and thermal power simultaneously, with higher thermal power and exergy compared to conventional photovoltaic thermal systems. For this purpose, a 3D transient numerical model is developed for investigating the system's performance in four main steps: (1) investigating the effects of the mass flow rate of the working fluid (20 to 50 kg/h) on the temperature behavior and thermodynamic performance of the system, (2) studying the impacts of using glass covers on the different parts of the system, (3) evaluating the annual energy and exergy analyses of the system under Mashhad weather conditions, and (4) examining the CO₂ reduction by using the proposed system. The results show that for the (glazed) PVT and (glazed) ST systems, increasing the mass flow rate of the working fluid from 20 to 50 kg/h results in 22% and 1.5% improvements in both thermal and electrical power, respectively. However, the thermal exergy of the system decreases by 40.1%. Furthermore, the (glazed) PVT/(glazed) ST systems generate approximately 86% and 264% more thermal power and energy than the PVT/ST systems, respectively. Using a (glazed) PVT/(glazed) ST system with a working fluid's mass flow rate of 50 kg/h results in maximum thermal and electrical efficiencies of 40.7% and 16.22%, respectively. According to the annual analysis, the highest average thermal and electrical power, equal to approximately 338.3 and 24 W, respectively, is produced in August. The amount of CO₂ reduction increases by increasing the mass flow rate and using a glass cover. The PVT/(glazed)ST system has the potential to reduce CO₂ emissions by 426.3 kg per year.

Keywords: Photovoltaic thermal system, solar thermal collector, environmental analysis, energy and exergy analyses, CO₂ reduction.

1. Introduction

Because of the world's fast population expansion and remarkable industrial progress, energy demand is significantly rising. Moreover, the traditional energy sources, fossil fuels, are responsible for today's global warming, air and water pollution, wildlife harm, etc. A prospective replacement for these energy sources are renewable energy sources such as wind, solar, and geothermal. Solar energy has received further

attention among the various kinds of renewable energy because it is limitless and widely available [1]. In the last two decades, two main solar systems have been introduced for converting solar irradiation into heat and electricity for use in different residential and industrial applications. Photovoltaic panels can generate electrical power, while solar thermal (ST) collectors convert the received solar irradiation into thermal power. Only a small amount of the sun's radiation can be converted by photovoltaic cells into electricity; the

This is an open access article under the [CC BY](https://creativecommons.org/licenses/by/4.0/) license:



remainder only raises the temperature of the photovoltaic cells, which reduces their electrical performance and shortens their lifespan [2]. Therefore, photovoltaic thermal (PVT) modules are used to solve the mentioned issues and recover the additional energy absorbed by photovoltaic cells [3]. In these systems, an ST collector is attached beneath the photovoltaic panel, where working fluid (WF) passes through the tubes/channels, resulting in a reduction in the temperature of the photovoltaic cells, an increase in the cells' efficiency, and the generation of thermal power [4]. Nevertheless, the frequent deployment usage of PVTs has significant restrictions due to some issues, namely, low WF outlet temperature, low thermal power, and exergy [5]. To tackle these problems and improve the performance of these systems, different enhancement methods are applied. As an example, some researchers have investigated the effects of adding nanofluids to WF [6], using turbulators through WF [7], employing phase change materials [8], a combination of these methods [1], and applying concentrators [9]. It should be mentioned that each improvement technique has its drawbacks. For example, nanofluids suffer from low improvements in low-volume fractions and possible settling and clogging in high-volume fractions [10]. Furthermore, the leakage problem and decrease in WF temperature once PCMs are used, as well as the high total and maintenance costs of concentrating photovoltaic thermal energy due to the complexity of the design, are issues with the mentioned methods [11]. Because PVTs have lower WF outlet temperatures, thermal powers, and exergies than STs, they are not used in high-temperature applications.

Recently, to resolve these problems, a hybrid system of PVT and ST (hybrid PVT/ST), connecting these two systems in series, has been introduced. In this system, the WF passes through the PVT system and then enters the ST section to increase the temperature to a suitable level for use in applications with a high required temperature. Ma et al. [12] introduced the hybrid PVT/ST system and numerically evaluated the performance of the system using a 2D model. Their investigations were conducted under the Shanghai, China, weather, where the lowest and highest amounts of electrical power were achieved in November and July, equal to 18.20 and 35.8 kWh, respectively. According to the annual analysis, the system could produce around 2096.51 and 298.50 kWh of thermal and electrical power, respectively. Li et al. [5] numerically studied the hybrid PVT/ST performance from energy and exergy viewpoints.

They applied a glass cover on top of two sections to investigate the effects of it on the system's performance. The 2D numerical model results illustrated that using the glass cover could improve thermal power to a maximum of 4.10 kWh. Moreover, using a glass cover decreased the electrical efficiency of cells due to the increase in cell temperature.

Han et al. [13] numerically compared the performance of two different systems, (1) a photovoltaic panel and ST collector that worked separately (the first system only produces electricity and the next one provides thermal power); and (2) a hybrid PVT/ST system. They conducted their simulations under a fixed heat flux and ambient temperature. They revealed that the hybrid PVT/ST system performed better under the higher solar heat flux and ambient temperature. The performance of four solar systems, including ST, photovoltaic panels, PVT, and hybrid PVT/ST, was studied by Kazemian et al. [14]. They developed a 3D numerical model and conducted their investigation under specific daytime weather conditions in July in Shanghai, China. They demonstrated that the mass flow rate was the main determinant of the system's thermal and electrical output, after solar irradiation and WF input temperature. The performance of a hybrid PVT/ST system with and without glass cover under the weather conditions of Chennai, India, was studied by Chandan et al. [15]. Using the glazed hybrid PVT/ST system increased the outlet temperature of the WF by 2-3 °C compared to the glazed PVT. Furthermore, the glazed hybrid PVT/ST system generated 23% less electrical power than the unglazed one.

Growing greenhouse gas emissions are one of the world's primary issues, resulting in significant environmental degradation. Due to the significance of carbon dioxide (CO₂) management in the modern world, it is essential to investigate the environmental effects of clean energy systems such as PVT/ST modules. Although some environmental analysis has been undertaken on PVT systems, such as that of Rajoria et al. [16], Hassani et al. [17], and Cetina-Quñones et al. [18], no research has been conducted on the hybrid PVT/ST system.

According to the literature, limited studies have been conducted to investigate the performance of the hybrid PVT/ST system. Only two studies investigated the annual performance of the PVT/ST system by only focusing on the energy viewpoint. Therefore, the annual performance of the system from an exergy viewpoint has not been investigated yet. Moreover, there is no study on the

environmental aspect of using hybrid PVT/ST systems. Consequently, considering both the first and second laws of thermodynamics in the analyses, the main objectives of this study can be summarized as follows:

- Studying how the WF mass flow rate in the range of 20–50 kg/h affects the temperature behavior and thermodynamic performance of the (glazed)PVT/(glazed)ST system.
- Evaluating the effects of glass cover on the system by defining various scenarios such as (glazed) PVT/(glazed) ST, PVT/(glazed) ST, and (glazed) PVT/ST.
- Analyzing the performance of the PVT/(glazed)ST system in an entire year from both energy and exergy standpoints.
- Examining the environmental effects of mass flow rate and glass cover on the PVT/(glazed)ST system, including the reduction in CO₂ pollutants and the annual reduction in CO₂,

Note that all the simulations are conducted under the weather conditions of Mashhad, Iran.

2. Numerical Modeling

2.1 Physical model

As indicated in Fig. 1, the hybrid PVT/ST system is comprised of two main sections: (1) a

photovoltaic thermal module, and (2) a solar collector system. The working fluid (WF) at the ambient temperature enters the PVT system and absorbs heat from the PV cells, resulting in a reduction in the PV cells' temperature and an increase in the WF outlet temperature. The heated WF, by passing through the connection tubes, enters the second section, the ST system, to increase the outlet temperature to the desired level. Fig. 1 also displays the different layers of the two sections. The PVT module includes a glass cover, PV cells with two layers of ethylene-vinyl acetate (EVA), Tedlar, an absorber plate, tubes containing WF, and insulation. Moreover, the solar collector includes a glass cover, an absorber plate, tubes containing WF, and insulation. It should be mentioned that the effect of using a glass cover on top of each part is studied, while in the figure, the (glazed) ST and PVT (unglazed) are the only ones shown. The air gap and glass cover prevent the transfer of heat to the surrounding environment. In numerical modeling, to reduce the cost and time of software-based calculations, only one tube is considered. The accuracy of this assumption has been proven in refs. [4, 19]. Table 1 lists the geometrical dimensions, whereas Table 2 lists the thermophysical and radiative parameters associated with the system. Water has been used as a WF in the present study.

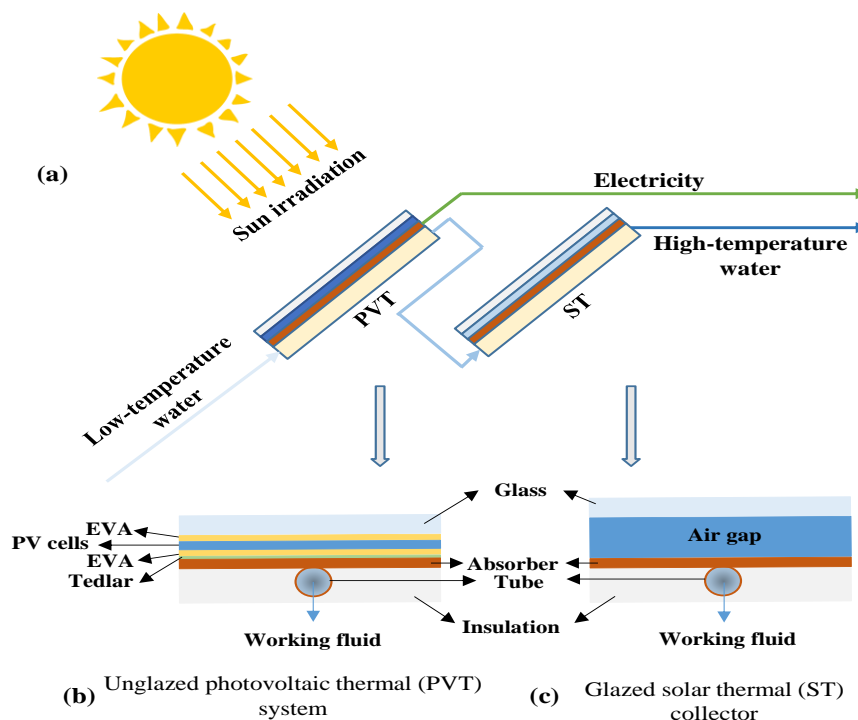


Fig. 1 (a) Schematics of the PVT/ST system along with cross-sectional views of (b) unglazed photovoltaic thermal (PVT) system and (c) glazed solar thermal (ST) collector with their various layers.

Table 1,
Dimensions of the PVT/ST system [4, 12].

System component	Dimensions (m)
The glass cover of the PVT and ST	2×0.1×0.0032
The absorber of the PVT and ST	2×0.1×0.004
Air gap	2×0.1×0.025
EVA	2×0.1×0.0005
Photovoltaic cells	2×0.1×0.0003
Tedlar	2×0.1×0.0001
Tube length of each part	2
Tube outlet diameter	0.1
Thickness of the tube	0.01

Table 2,
Thermophysical and radiation properties of the different elements [4, 12].

System component	Density (kg/m ³)	Conductivity (W/m.K)	Specific heat (J/kg.K)	Transmittance	Absorptance
Glass cover	2200	0.76	830	0.95	0.02
EVA	960	0.35	2090	1	0
Photovoltaic cells	2330	148	700	0	0.92
Tedlar	1200	0.2	1250	-	-
Absorber plates and tubes	8960	401.00	385	0	0.95

2.2 Assumptions

In this research, assumptions have been considered to solve the equations and decrease some complexity in modeling. The laminar flow regime is considered due to the Reynolds number being less than 2300 and the maximum mass flow rate of 50 L/h considered in this study [20]. The anti-reflection coating layer for the PV cells has a very small thickness (0.0001 mm), so it is omitted in this numerical study. Moreover, the contact resistance between the layers is assumed to be negligible. The thermal properties of all materials are constant and do not change with temperature changes. To simulate the input radiation, it is assumed that the radiation is uniform and perpendicular to the surfaces of the two parts of the system.

2.3 Governing equations

For the solid parts (subscript “s”) of both PVT and ST components, the conduction heat transfer is as follows [14]:

$$(\rho_s c_{p,s}) \frac{\partial T_s}{\partial t} = \nabla \cdot (k_s \nabla T_s) + E''_{sun\ eff,PV\ or\ abs} - E''_{el} \quad \dots(1)$$

T_s , ρ_s , $c_{p,s}$ and k_s are the temperature, density, specific heat, and thermal conductivity, respectively. Moreover, $E''_{(sun\ eff,PV\ or\ abs)}$ and E''_{el} indicate the effective energy

absorbed by PV cells and absorber plate and the electric power produced in the PV cells, respectively. It is clear that the second term is zero for all other layers. These source terms can be calculated by the following relations [4, 12]:

$$E''_{sun\ eff,PV\ or\ abs} = \tau_{glass} \alpha_{PV\ or\ abs} I_{sun} \quad \dots(2)$$

$$E''_{el} = E''_{sun\ eff,PV} \eta_r [1 - 0.0045(T_{cell} - 298.15)] \quad \dots(3)$$

Using user-defined function (UDF) codes, these source terms are applied to the numerical simulation. In these equations, τ_{glass} is the transmission coefficient of the glass, $\alpha_{(PV\ or\ abs)}$ is the absorptivity coefficient of the PV cells or absorber plate, I_{sun} is the solar irradiation, and η_r is the reference efficiency of the PV cell, which is equal to 0.173.

The continuity, momentum, and energy equations for fluid (WF and air) are given as follows [21]:

$$\vec{\nabla} \cdot (\rho_f \vec{V}_f) = 0 \quad \dots(4)$$

$$\vec{\nabla} \cdot (\rho_f \vec{V}_f \vec{V}_f) = -\vec{\nabla} P + \vec{\nabla} \tau_1 + \rho_f \vec{g} \quad \dots(5)$$

$$\vec{\nabla} \cdot (\rho_f c_{p,f} T_f \vec{V}_f) = \vec{\nabla} \cdot (k_f \vec{\nabla} T_f) \quad \dots(6)$$

\vec{V}_f and P present fluid velocity and pressure, respectively, and subscript “f” stands for both fluids of WF in the tube and air inside the gap.

2.4 Boundary conditions

The boundary conditions of the inlet and outlet are set to mass flow inlet and pressure outlet, respectively. Moreover, the adiabatic walls are applied to the lateral sides, tube, and absorber plates of both components of the system. To calculate the amounts of radiation and convection heat transfer to the environment, the convection heat transfer coefficient and the sky temperature are calculated by [22, 23]:

$$T_{sky} = 0.0552T_{amb}^{1.5} \quad \dots(1)$$

$$h_{wind} = \begin{cases} 5.7 + 3.8V_{wind} & \text{if } V_{wind} < 5 \frac{m}{s} \\ 6.47 + V_{wind}^{0.78} & \text{if } V_{wind} \geq 5 \frac{m}{s} \end{cases} \quad \dots(2)$$

V_{wind} and T_{amb} are wind velocity and ambient temperature, respectively.

2.5 Performance evaluation method

The thermal power of the system is calculated by [14]:

$$\dot{E}_{th} = \dot{m}_f c_{p,f} (T_{f,out} - T_{f,in}) \quad \dots(9)$$

where \dot{m}_f , $T_{f,out}$, and $T_{f,in}$ are mass flow rate, and WF temperatures at the inlet and outlet, respectively. To calculate thermal and electrical efficiencies, the following equations can be used, respectively [5]:

$$\eta_{th} = \frac{\dot{E}_{th}}{(\tau_{glass} \alpha_{pv} A_{pv} I_{sun}) + (\tau_{glass} \alpha_{abs} A_{abs} I_{sun})} \quad \dots(10)$$

$$\eta_{el} = \frac{E''_{el}}{\tau_{glass} \alpha_{pv} I_{sun}} \quad \dots(11)$$

where, A_{pv} and A_{abs} are the surface area of PV cells and absorber plate, respectively. Using the

following equations, the rate of electrical and thermal exergy can be calculated [24]:

$$\dot{E}_{x_{el}} = E''_{el} \times A_{pv} \quad \dots(6)$$

$$\dot{E}_{x_{th}} = \dot{m}_f c_{p,f} \left((T_{f,out} - T_{f,in}) - T_{amb} \ln \left(\frac{T_{f,out}}{T_{f,in}} \right) \right) \quad \dots(7)$$

2.6 Environmental analysis: CO₂ reduction

The usage of renewable energy minimizes carbon dioxide (CO₂) emissions caused by the burning of fossil fuels. Therefore, the amount of this reduction by using the proposed system is studied. It should be noted that the amount of carbon dioxide reduction can be obtained from the two points of view of energy and exergy, whose general relations are the same. The amount of carbon dioxide reduction (kg per month/year) can be calculated as follows [16]:

$$\Phi_{CO_2} = \beta_{CO_2} \times \dot{E}_{eq,total} \quad \dots(8)$$

$\dot{E}_{eq,total}$ is the total amount of energy produced by the system, including electrical and thermal power by taking into account the power plant efficiency of 38% as follows [16]:

$$\dot{E}_{eq,total} = (\dot{E}_{el} + 0.38 \times \dot{E}_{th}) \times n / 1000 \quad \dots(9)$$

In this equation, n represents the total monthly operating hours for the city of Mashhad, as depicted in Fig. 2. The quantity of n is determined based on the number of sunny days in a month (using the data provided by [25]) and operating hours of the system, which is considered 8 hours per day in this study. In Eq. (14), β_{CO_2} is the amount of CO₂ production per coal consumption to produce a kW of useful power, which is usually considered equal to 2 [16].

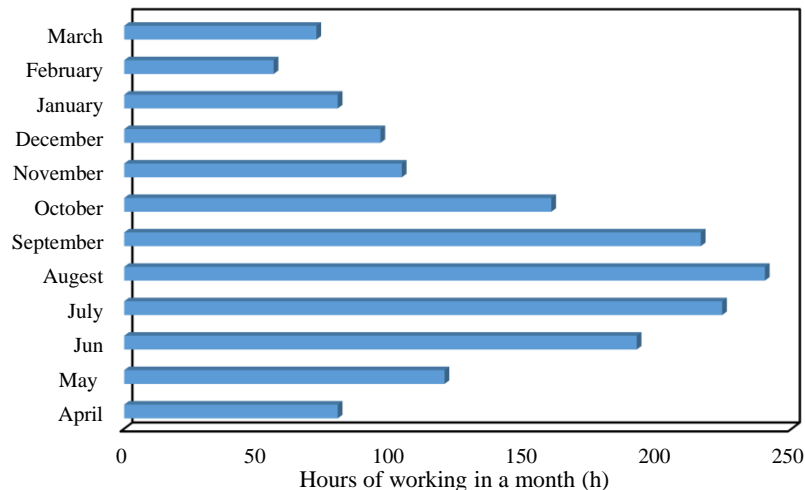


Fig. 2. The total number of working hours per month in Mashhad [25].

2.7 Numerical simulation procedure

Using ANSYS Fluent version 18.2, a 3D transient numerical model is developed for evaluating the performance of the PVT/ST system. The pressure-based solver is employed for the laminar regime of WF, and the SIMPLE method is used to couple pressure and velocity. The second-order upwind is used for discretizing different terms in all governing equations, while the PERESTO scheme is employed for the pressure [26, 27]. Furthermore, in solving continuity, momentum, and energy equations, convergence criteria of 10^{-6} , 10^{-6} , and 10^{-8} are considered, respectively.

2.8 Grid and time-step independence study

In this section, two important parameters affecting the numerical solution, including the number of grids and time step, have been

investigated. The geometry of the PVT/ST is generated in SolidWorks software, and then a structural mesh is provided for the computational domain using ANSYS meshing software. Fig. 3(a) illustrates the structural grid system used for the PVT part of the system. Fig. 3(b) and (c) show the results of grid and time-step independence when two parameters are considered: WF outlet temperature and thermal power. Four grids of 605000, 1270000, 2650000, and 5150000 are considered. Comparing the data for the 605000 and 1270000 grids with the 5150000 grids reveals errors of approximately 10% and 6%, respectively. Nonetheless, the error for 2650000 grids is approximately 1.5% compared to the case with 5150000 grids. As a result, the grid system with 2650000 grids is chosen for the remainder of the research. Finally, at the selected grid system, the effects of applying different time steps of 17, 35, 70, and 140 s on the two considered parameters are compared, as shown in Fig. 3(c). Regarding both calculation speed and accuracy of results, a time step of 70 s was chosen for this study.

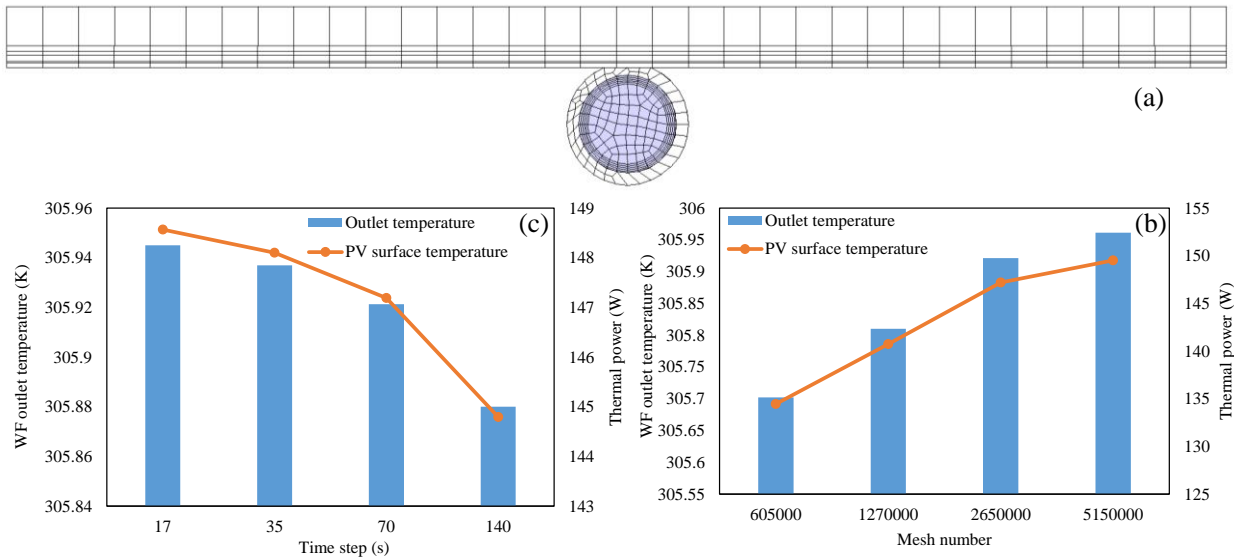


Fig. 3 (a) Sample of the structural grid system used for the PVT part of the system along with investigating the independence of (b) grid number and (c) time-step.

3. Model Validation

To ensure that the results of the numerical study are accurate, the outputs of the present modeling for a PVT/ST system are compared with the experimental data provided by Chandan et al. [15]. Their PVT section consisted of 70 cells with an aluminum collector with 12 straight tubes (with an outer diameter and thickness of 16 and 0.5 mm, respectively). The ST section was made of copper with nine straight tubes (with an outer diameter and thickness of 12 and 0.5 mm, respectively). The length and width of both sections were equal—2 and 1 meters, respectively. The bottom surfaces of

both systems were insulated by glass wool with a thickness of 50 mm. Other geometrical and thermophysical properties of layers are available in ref. [15].

Fig. 4 illustrates the thermal and electrical power generated by the ST and PVT sections of the system, calculated by the numerical model and presented by Suresh et al. [15]. The experiments were conducted under the weather conditions of Chennai, India, at a flow rate of 30 l/h. According to the figure, the average errors for electric and thermal power are about 2.5% and 2.3%, respectively, which shows that the experimental and numerical results are in good agreement.

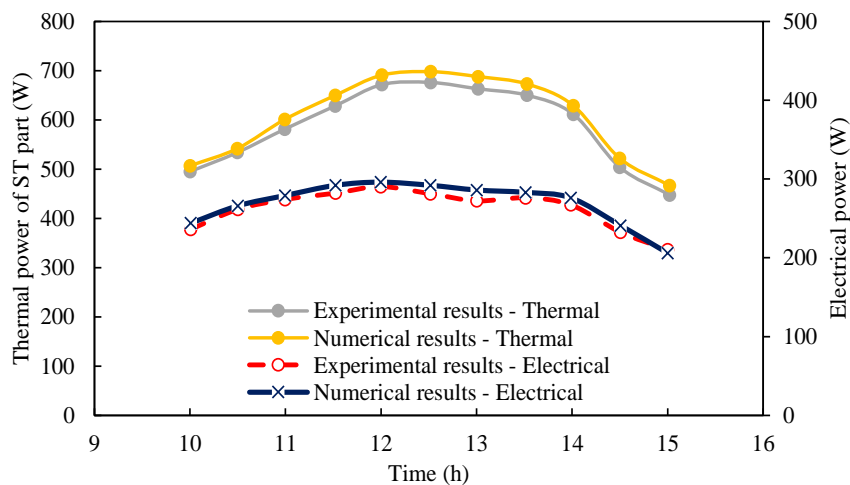


Fig. 4 Comparing the thermal and electrical power calculated by using the numerical model with the experimental data reported by Suresh et al. [15].

4. Results and Discussion

This study is presented in different sections. First, the effects of mass flow rate on the performance of the system have been explored. Next, the impacts of the glass cover on the different parts of the system are discussed. These sections are carried out under the August weather conditions of Mashhad, Iran. Then, the yearly performance of the system is presented for both

energy and exergy. Finally, an environmental analysis is presented, considering the effects of flow rate and glass cover. The variations of the average hourly solar irradiation and ambient temperature in a whole year in Mashhad, Iran, along with the average wind speed for each month, are plotted in Fig. 5 [28]. Note that the weather conditions vary during the day; therefore, by utilizing UDF, these conditions have been applied in the software.

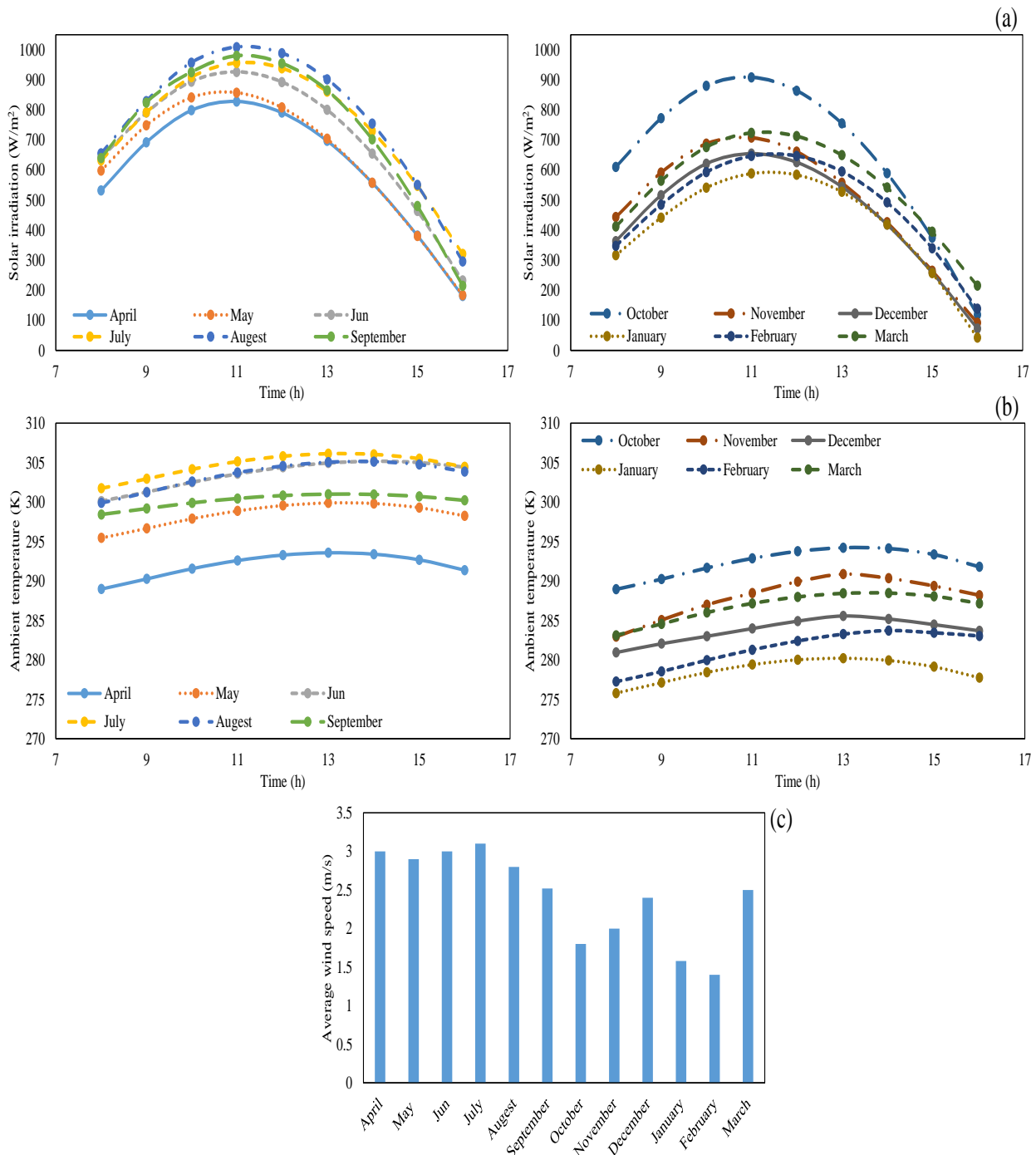


Fig. 5. Average hourly variations of (a) solar irradiation, (b) ambient temperature in a whole year in Mashhad, and (c) average wind speed for each month [28].

4.1 Effect of working fluid mass flow rate on the system performance

Figures 6(a) and (b) show the hourly temperature changes at the PV surface and the WF outlet from 8:00 to 16:00 for four different mass flow rates of 20, 30, 40, and 50 kg/h (laminar regime). It should be noted that the investigations are carried out on a typical day in August for the system, whose two parts are covered by a glass cover (glazed PVT and glazed ST). According to the graph, regardless of mass flow rate, as solar irradiation and ambient temperature rise due to the system's absorption of more heat, the surface temperature and WF outlet temperature rise. For example, at a flow rate of 20 kg/h at around noon, the system has the highest temperatures in the cells and the WF outlet, which are, respectively, 318.6 and 322 K.

By increasing the mass rate of the WF from 20 to 50 kg/h, the heat transfer coefficient in the flow increases, and as a result, the heat transfer from the surface that absorbs solar irradiation to the WF also increases. Therefore, based on Fig. 6(a), due to the

increment in absorbing heat from the system, the temperature of the PV surface decreases. It is worth mentioning that lowering the surface temperature helps to improve the useful lifespan and electrical efficiency of the PV cells. On the other hand, the results show that the increase in the mass rate leads to a reduction in the WF outlet temperature (see Fig. 6(b)), which is because of the decline in WF residence time in the tube. By increasing the mass flow rate from 20 to 50 kg/h, the PV surface temperature and the outlet temperature decrease on average by 3.2 and 7.4 K, respectively. To better understand the temperature distribution on the PV surface, Fig. 7 is plotted, which shows the contours of PV surface temperature at different WF mass flow rates during a day in August. Based on these contours, the inlet point experiences the lowest temperature, while by moving toward the flow direction to the end, the PV surface temperature increases. This is due to the weakening of the WF's ability to absorb heat. However, by raising the mass flow rate, we can successfully reduce this higher temperature at the end of the PVT part, especially at noon, when the maximum solar irradiation is available.

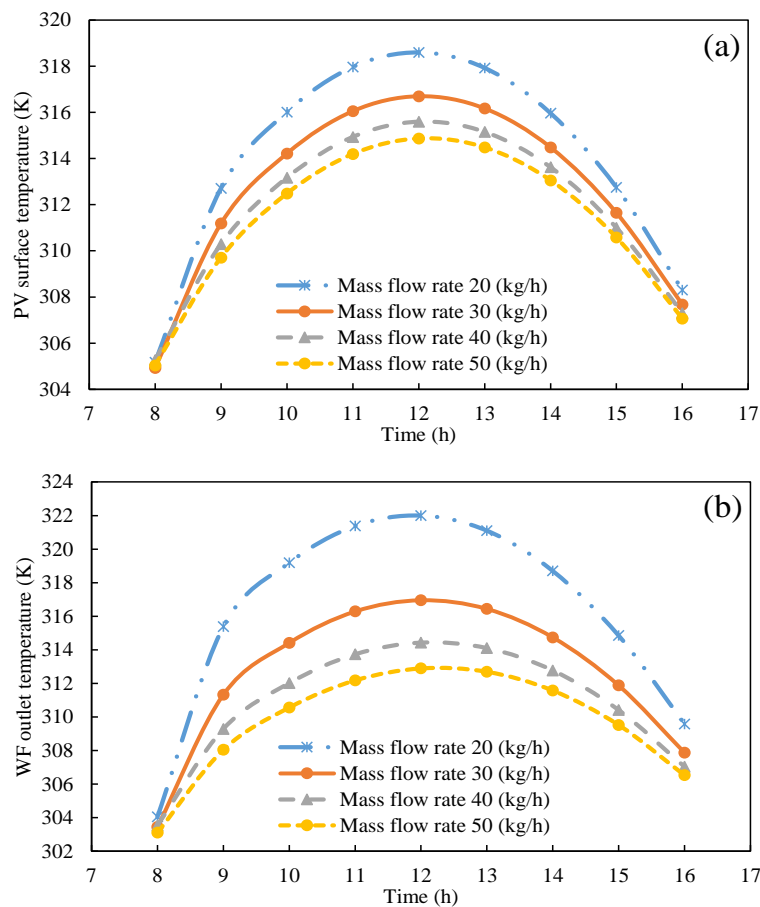


Fig. 6. Temporal variations of the (a) PV surface temperature and (b) WF outlet temperature at different mass flow rates during a day in August.

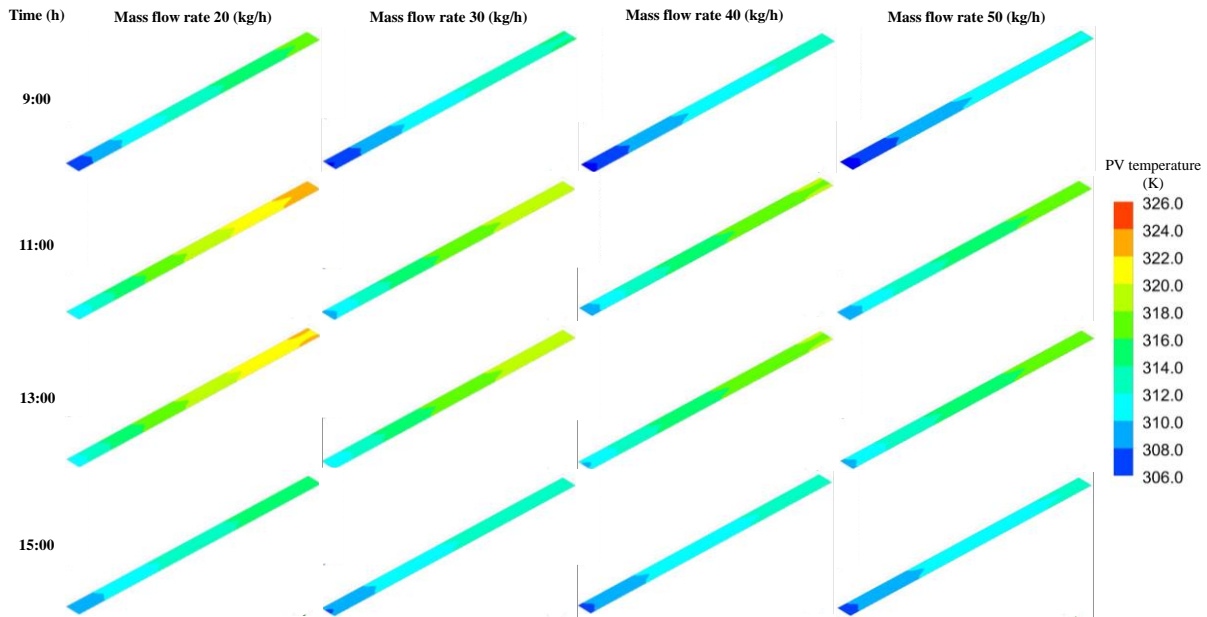


Fig. 7. Contours of PV surface temperature at different WF mass flow rates and time during a day in August.

The performance of the PVT and ST has been investigated from the perspectives of energy and exergy. Figures 8(a) and (b) show the temporal variations in thermal power and rate of energization at different mass flow rates during an August day. Despite the decrease in outlet temperature, the thermal power increases with an increase in the mass flow rate of the WF, which indicates the dominance of the flow rate increment over the reduction in the outlet temperature. In spite of the reduction in outlet temperature due to the increase in WF mass flow rate, the amount of heat absorption becomes higher, leading to an increase in the thermal power of the system. From the standpoint of exergy, as the mass flow rate

increases, the rate of thermal exergy decreases. According to Eq. (11), besides the mass flow rate and inlet and outlet temperatures, the thermal energy depends on the ambient temperature. In fact, by decreasing the outlet temperature, the temperature difference between the WF temperature and the ambient temperature decreases, causing a decrease in energy. Raising the mass flow rate of the WF from 20 to 50 kg/h, the daily average of thermal power increases by about 65.33 W, which is equivalent to approximately a 22% improvement (see Fig. 8(a)). On the other hand, this increase in mass flow rate causes the average daily thermal exchange rate to drop by about 40.1% (see Fig. 8(b)).

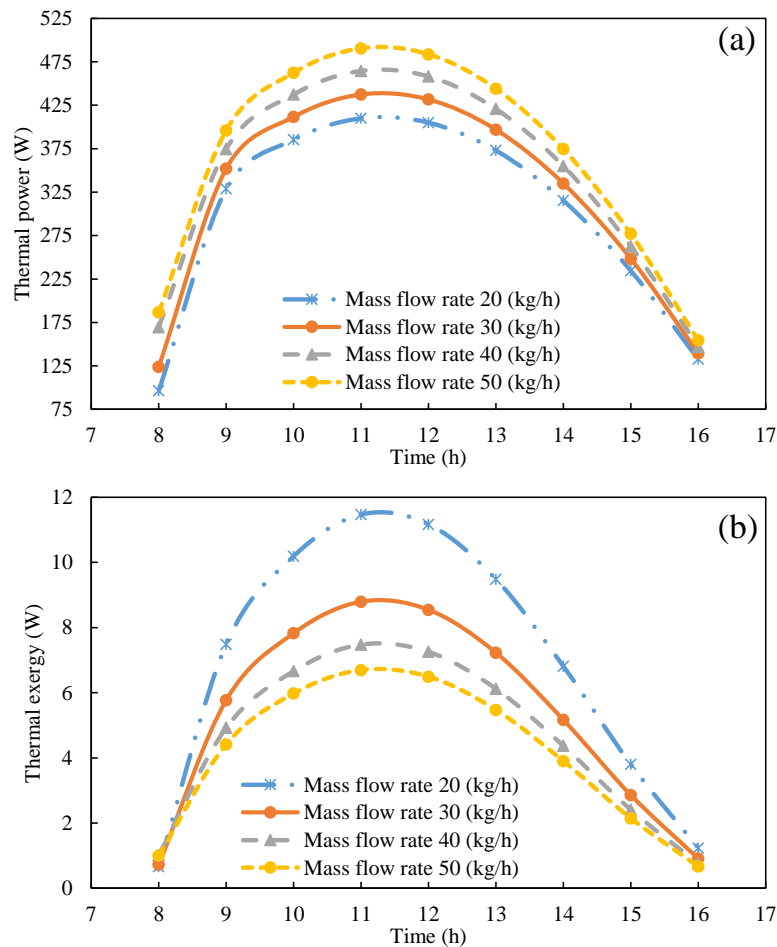


Fig. 8. Temporal variations of the (a) thermal power and (b) rate of thermal exergy at different mass flow rates during a day in August.

As mentioned earlier, increasing the WF mass flow rate leads to a reduction in the PV surface temperature. The cells' temperature has an inverse relationship with the electrical power, where its reduction improves the electrical performance of the system in terms of both energy and exergy, as shown in Fig. 9. According to the results, the maximum electrical power generated by the system at the peak of solar irradiation for mass flow rates of 20 and 50 kg/h is about 27.2 and 27.7 W, respectively. Considering the average electrical power produced during the day, using a mass flow rate of 50 kg/h improves the generated electricity by about 1.5% compared to the lowest amount of mass flow rate. Moreover, based on Eq. (12), the whole electrical power is considered useful energy; therefore, the electrical energy and exergy are the

same. Finally, according to the results presented in this section, a mass flow rate of 50 kg/h is selected for the rest of the investigations.

Fig. 10 demonstrates the average thermal and electrical efficiencies of the (glazed) PVT/(glazed) ST system at different mass flow rates throughout the course of a day in August. Based on the earlier discussion, the mass flow rate of 50 kg/h possesses the highest thermal and electrical powers. Consequently, at this mass flow rate, the system reflects maximum thermal and electrical efficiencies of 40.7% and 16.23%, respectively. These efficiencies are 2.65% and 0.13% higher than the efficiencies produced once the mass flow rate of 20 kg/h is used.

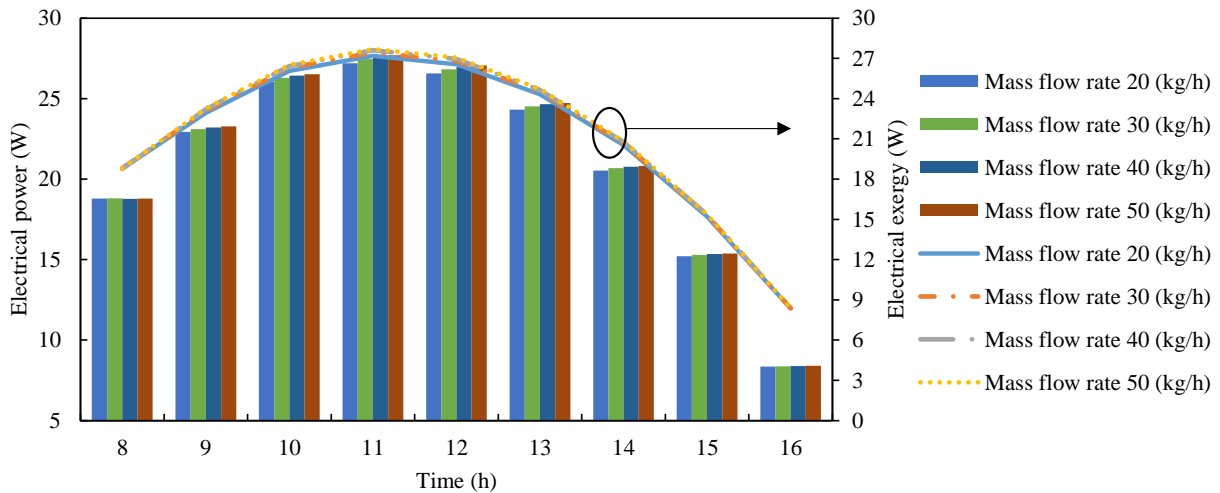


Fig. 9. Temporal variations of the electrical power and rate of electrical exergy at different mass flow rates during a day in August.

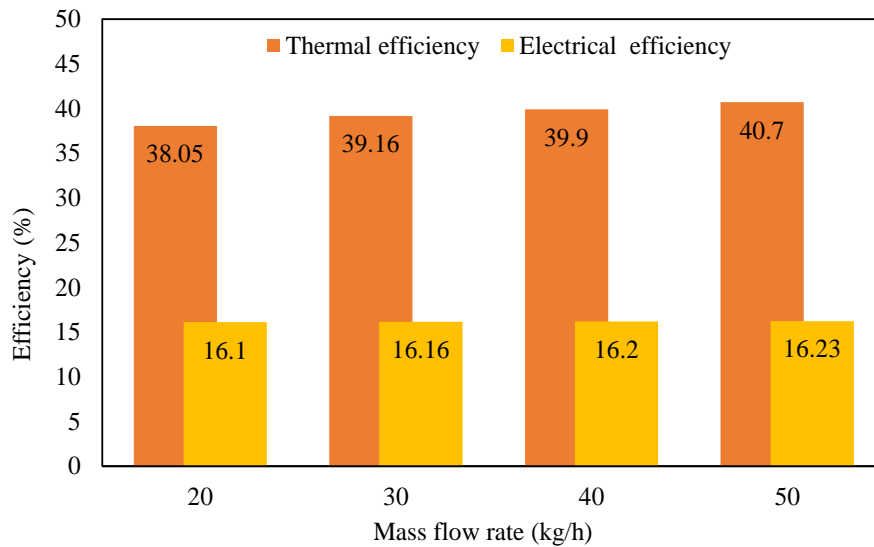


Fig. 10. Average thermal and electrical efficiencies of (glazed)PVT/(glazed)ST system at different mass flow rates during a day in August.

4.2 Effect of using glass cover on different sections of the system

The installation of a glass cover at the top of each system section, namely, PVT and ST, traps heat within the system, thereby reducing heat loss to the environment and enhancing thermal efficiency [4]. Therefore, in this section, the effect of using glass in two different parts of the PVT/ST system is investigated. For this purpose, four different modes are considered, including a system without a glass cover (PVT/ST), an all-glass system (glazed) PVT/(glazed) ST, only the PVT part with a glass cover (glazed) PVT/ST, and only the ST part with a glass cover (PVT/(glazed) ST). Figures 11(a) and (b) depict the temporal variations

of the PV surface and WF outlet temperatures for different PVT and ST with and without glass cover on various parts on an August day at a mass flow rate of 50 kg/h. Regarding Fig. 11(a), the PVT with a glass cover (glazed PVT) has the highest surface temperature due to the greenhouse effect between the cover and the PV cells inside the air gap; consequently, removing the glass reduces the surface temperature of the solar cell. On average, if a glass cover is used in the PVT system, the surface temperature increases by about 2.6 K compared to the case without a glass cover. However, removing the glass from the PVT part reduces the WF outlet temperature. Comparing the effects of using a glass cover on two parts on the outlet temperature, the glass has the greatest effect on the ST section,

where the removal of the glass has caused a further decrease in the temperature of the WF outlet, as can be seen in Fig. 11(b). As a result, the lowest temperature of the outlet fluid belongs to the

PVT/ST system. If the glass cover is used in both parts, (glazed) PVT and (glazed) ST, the WF outlet temperature increases by about 2.35 K compared to the case without the glass cover.

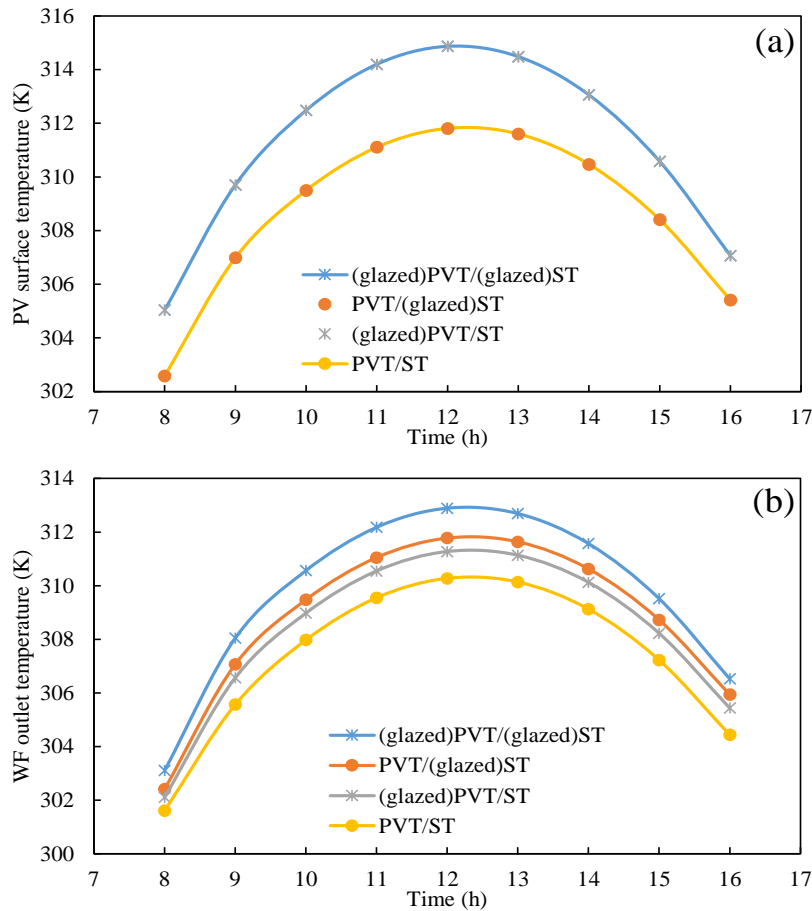


Fig. 11. Temporal variations of the (a) PV surface temperature and (b) WF outlet temperature for different PVT/ST with and without glass cover on various parts at the mass flow rate of 50 kg/h during a day in August.

The average thermal and electrical power and efficiency for various PVTs and STs with and without glass covers at a mass flow rate of 50 kg/h during an August day are depicted in Figs. 12(a) and (b). Fig. 12(a) shows that if both components are equipped with a glass cover, the highest thermal power and the lowest electrical power are obtained. The glazed PVT/ST system has the ability to produce about 86% more thermal power than the system without a glass cover. But on the other hand, if the glass is used on the PVT part, the electrical power decreases by about 1.5 W due to the increase in cell temperature. The PVT/ST system in which the ST section is equipped with a glass cover improves its thermal power by 71.7 W (equal to about 26.9%) compared to the combined system in which the PVT section is equipped with a glass cover. According to Fig. 12(b), using a glass

cover on top of the ST part has a greater effect on thermal efficiency compared to the PVT part. For instance, implementing glass in the ST part increases the thermal efficiency by 11.95% in comparison with the PVT/ST system, while employing glass in the PVT part only increases the thermal efficiency by 2.28%. The maximum improvement of 14.4% can be achieved once both parts are covered by glass. Moreover, the effect of using a glass cover on average electrical efficiency is minimal.

Fig. 13 depicts the average rate of thermal and electrical energy for different PVTs and STs with and without glass covers at a mass flow rate of 50 kg/h during a day in August. The results show that the (glazed) PVT/(glazed) ST system has the highest rate of thermal exchange, which is 264% greater than the PVT/ST system. However, adding

a glass cover to the PVT part reduces the rate of electrical energy. Furthermore, the effect of using a glass cover in the ST part is more pronounced than in the PVT part, with the PVT/(glazed)ST system having 67% more thermal energy than the (glazed)PVT/ST system.

According to the results presented in this section, in order to achieve maximum electrical power, a system without glass in the PVT section should be used, while the presence of glass in the ST section increases the thermal power significantly. As a result, the PVT/(glazed)ST system is chosen for additional research.

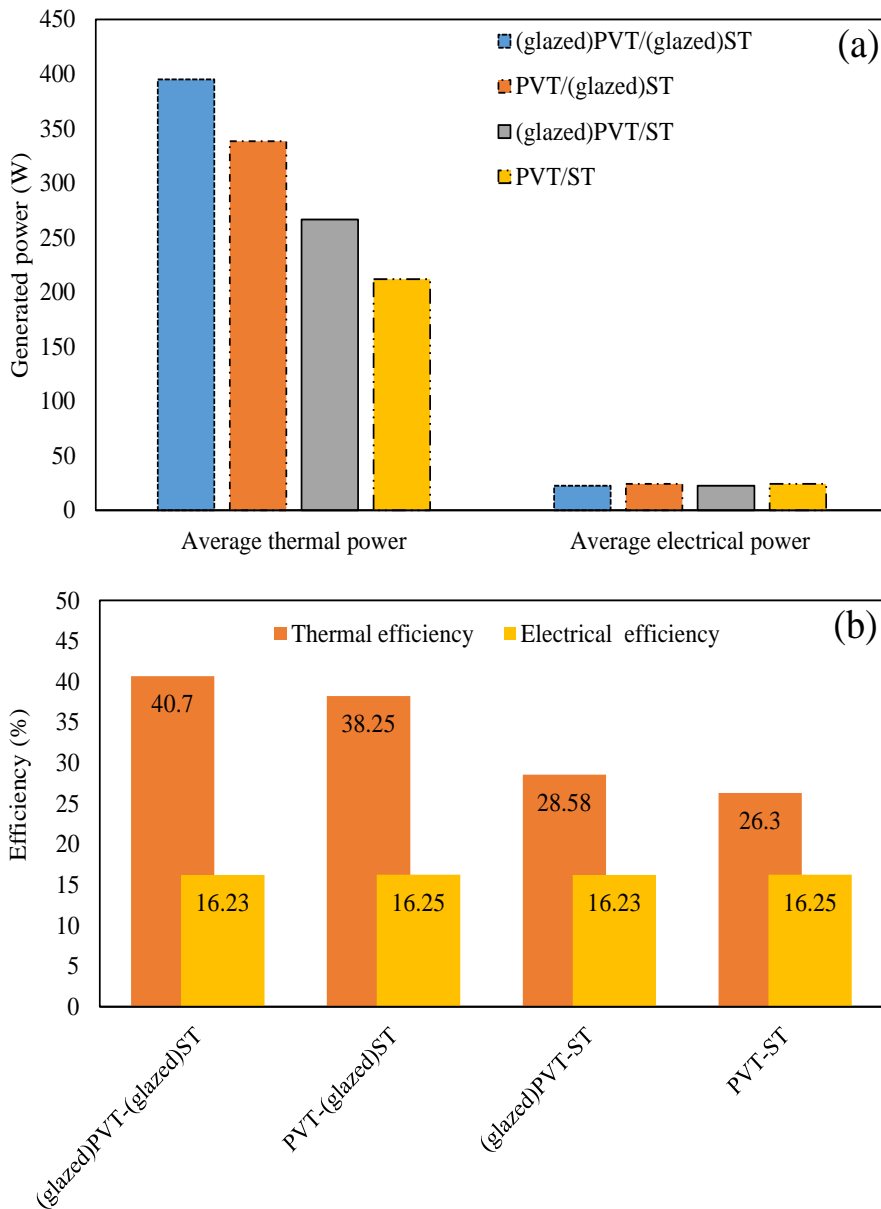


Fig. 12. Average thermal and electrical (a) power and (b) efficiencies for different PVT/ST with and without gl cover on various parts at the mass flow rate of 50 kg/h during a day in August.

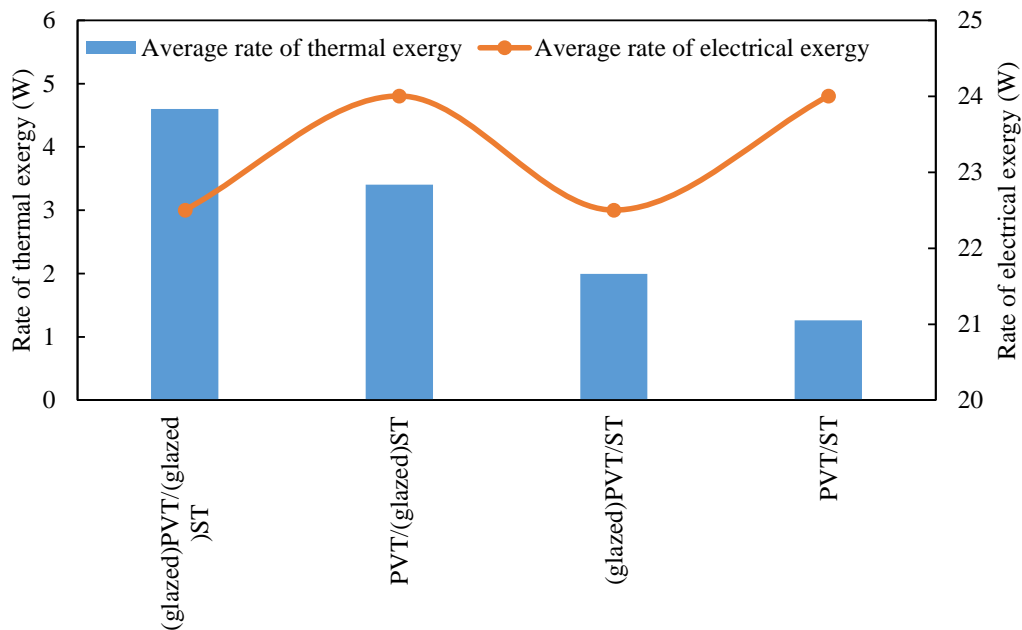


Fig. 13 Average rate of thermal and electrical exergy for different PVT/ST with and without glass cover on various parts at the mass flow rate of 50 kg/h during a day in August.

4.3 Yearly performance of the system

According to the weather conditions reported at the beginning of the results section, the performance of the PVT/(glazed)ST system for the selected mass flow rate of 50 kg/h is presented in Fig. 15 for a typical day in each month. As seen in Fig. 15(a), both thermal and electrical power are at their peaks in the summer due to both sections of the system's ability to collect more solar energy. Therefore, the highest average thermal and electrical power produced by the system occurs in

August, which is equivalent to about 338.3 and 24 W, respectively, because of the high radiation and ambient temperature in this month. On the other hand, due to the severe decrease in ambient temperature and solar irradiation in January, the system produces the lowest average thermal and electrical power of roughly 180.4 and 14.9 W, respectively. Similar results can be observed for the rate of thermal and electrical exergy, as shown in Fig. 15(b), where the highest rate of exergy is obtained in summer and the lowest rate in winter.

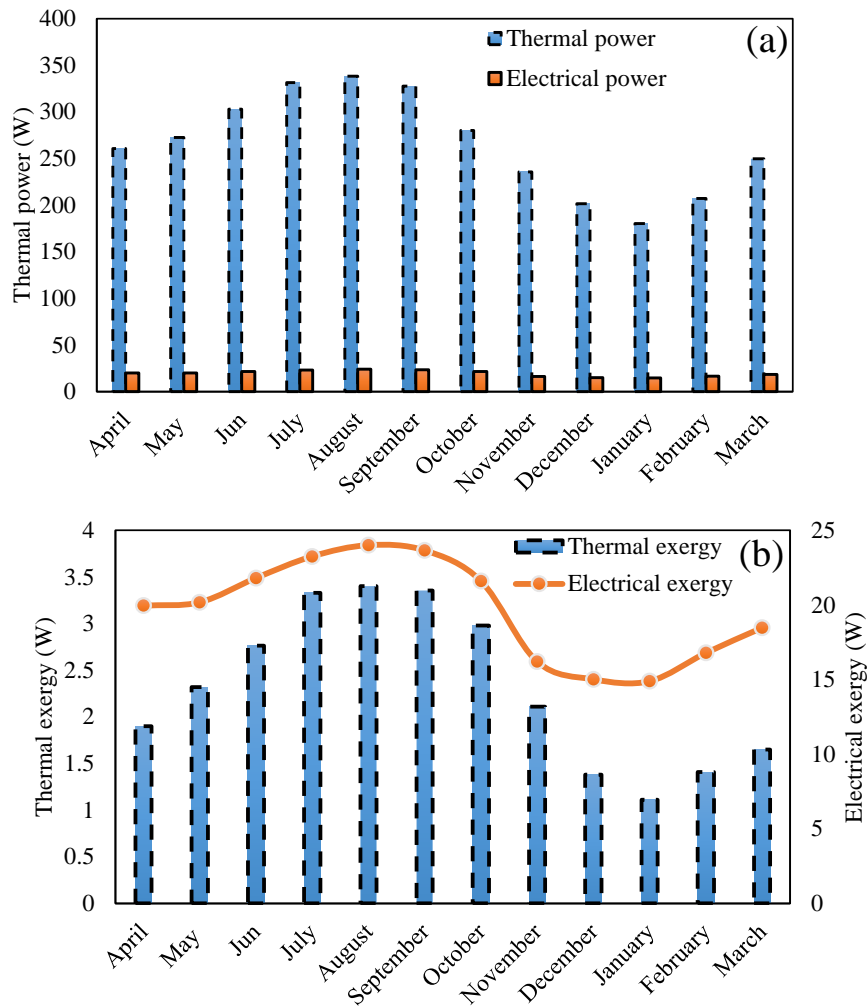


Fig. 14. Monthly performance of the PVT/(glazed)ST system from (a) energy and (b) exergy viewpoints.

4.4 Environmental analysis: CO₂ reduction

As one of the most prominent greenhouse gases, CO₂ has crucial impacts on global climate change and air pollution. Consequently, using a clean energy system like the one proposed in this study can reduce the production of CO₂. Using Eq. (14) and based on the calculated thermal and electrical power in previous sections, the amounts of CO₂ reduction for different cases are determined. In a typical August day, Figs. 15(a) and (b) show the amount of CO₂ reduction for the (glazed) PVT and (glazed) ST systems at different mass flow rates, as well as four different PVT and ST systems with and without glass covers (presented in Section 4.2). By increasing the WF mass flow rate, the amount of CO₂ reduction increases due to the increment in both the thermal and electrical power of the system. For example, using the system at a mass flow rate of 20 kg/h reduces CO₂ by approximately 70.7 kg, while increasing the mass flow rate to 50 kg/h

increases this amount by 12.1 kg (a 17.1% improvement as shown in Fig. 15(a)).

As discussed earlier, using a glass cover dramatically increases the thermal power of both the PVT and ST sections, while negatively affecting the electricity produced by the PV cells. As a result, the maximum and minimum CO₂ reductions belong to the (glazed) PVT/(glazed) ST and PVT/ST systems, as shown in Fig. 15(b), where the amount of CO₂ emission reduces from around 82.8 to 50.15 kg (a 39.4% decrease in CO₂ reduction). Furthermore, using (glazed) PVT/ST and PVT/(glazed) ST systems could reduce CO₂ emissions by approximately 73.2 and 59.4 kg, respectively. It should be noted that the PVT/(glazed)ST system is chosen for monthly performance evaluation because of its superior electrical performance, despite having a lower CO₂ reduction than the PVT/(glazed)ST system.

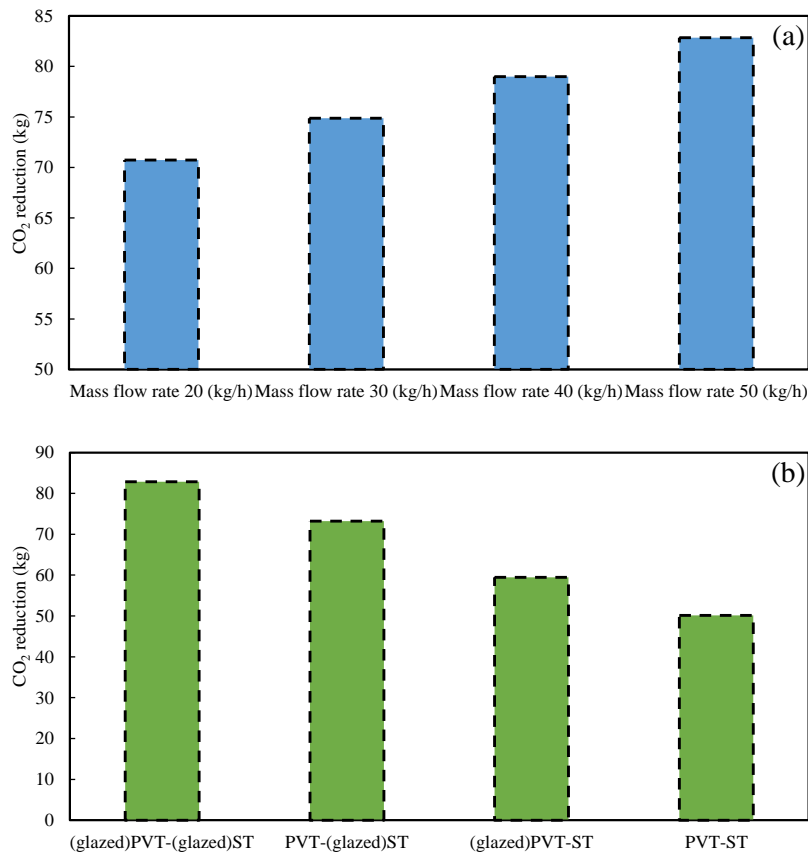


Fig. 15. CO₂ reduction for (a) (glazed)PVT/(glazed)ST system at different mass flow rates and (b) four differ PVT/ST systems with and without glass cover on a typical day in August.

Finally, Fig. 16 depicts the CO₂ reduction on a typical day of each month for the PVT/(glazed)ST system at a mass flow rate of 50 kg/h. Since the total average power of the system has a direct relationship with the reduction of CO₂, the highest amount of CO₂ reduction can be absorbed in August, which is followed by July and September. On the other hand, the lowest value of CO₂ reduction is not achieved in January (the lowest

thermal and electrical production occur in this month, as illustrated in Fig. 15(a)). Due to the lower sunny days [25], it belongs to February by 10.7 kg, and as a result, the total working hours reported for this month in Fig. 2. Ultimately, using the PVT/(glazed)ST system can reduce CO₂ emissions by 426.3 kg per year.

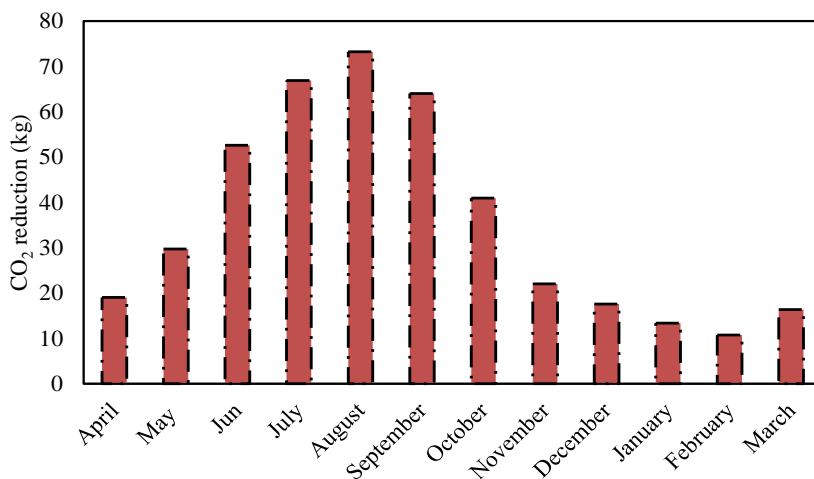


Fig. 16. Monthly CO₂ reduction for PVT/(glazed)ST system at the mass flow rate of 50 kg/h on a typical day in months.

5. Conclusion

The performance of a hybrid system called PVT/ST, which consists of a photovoltaic thermal module and a solar flat collector connected in series, was investigated in this study. To investigate the annual performance of the system from energy, exergy, and environmental perspectives, a numerical simulation was conducted by considering the weather conditions in Mashhad, Iran. Moreover, the effects of the working fluid mass flow rate (20–50 kg/h) and the influence of using a glass cover on each part of the PVT/ST system were investigated in August. Finally, the effects of these parameters on CO₂ reduction were discussed. The results of this research indicate:

- By increasing the working fluid's mass flow rate from 20 to 50 kg/h in the (glazed) PVT/(glazed) ST system, both the PV surface temperature and the working fluid's outlet temperature decreased by an average of 3.2 and 7.4 K, respectively, improving both thermal (22%) and electrical (1.5%) power. However, with this increment in mass flow rate, the thermal entropy decreased by 40.1%.
- The glazed PVT/ST system generated approximately 86% and 264% more thermal power and energy than the PVT/ST system. Due to the increase in temperature of the PV cells, using a glass cover on the PV component decreased the electrical power by about 1.5 W.
- The systems in August and January could produce the highest and lowest average thermal powers, approximately 338.3 and 180.4 W, respectively. Furthermore, the generated electricity for these months was 24.9 and 14.9 W, respectively.
- The CO₂ reduction increased as the mass flow rate rose due to an increase in both the system's thermal and electrical power, e.g., increasing the mass flow rate from 20 to 50 kg/h improved the amount of CO₂ reduction by approximately 17.1%. Moreover, using glazed PVT or glazed ST instead of PVT or ST enhanced the amount of CO₂ reduction by 39.4%. Finally, employing PVT or (glazed) ST systems could reduce the production of CO₂ by 426.3 kg in a year.

Nomenclature

A	Area (m ²)
c_p	Specific heat capacity (J/kg.K)
$\dot{E}x$	Rate of exergy (W)
\dot{E}	Power (W)
h	Convection heat transfer coefficient (W/m ² .K)
I	Solar irradiation (W/m ²)
k	Thermal conductivity coefficient (W/m.K)
\dot{m}	Mass flow rate (kg/s)
P	Pressure (Pa)
T	Temperature (K)
t	Time (s)
V	Velocity (m/s)

Greeks

ρ	Density (kg/m ³)
α	Absorptivity
η	Reference of energy efficiency (%)
τ_g	Glass transmissivity
μ	Dynamic viscosity (kg/m.s)
ϕ	The yearly CO ₂ reduction

Subscripts

abs	Absorber
amb	Ambient
el	Electrical
eq	Equivalent
eff	Effective
f	Fluid
in	Inlet
out	Outlet
pv	Photovoltaic cell
s	Solid
th	Thermal

Abbreviation

EVA	Ethylene-vinyl acetate
PV	Photovoltaic unit
PVT	Photovoltaic thermal module
PVT/ST	Hybrid photovoltaic thermal system and solar thermal collector
ST	Solar thermal collector
WF	Working fluid

6. References

- [1] A. Kazemian, M. Khatibi, S.R. Maadi, T. Ma. Performance optimization of a nanofluid-based photovoltaic thermal system integrated with nano-enhanced phase change material. *Applied Energy*. 295 (2021) 116859.
- [2] S.K. Pathak, P.O. Sharma, V. Goel, S. Bhattacharyya, H.Ş. Aybar, J.P. Meyer. A detailed review on the performance of photovoltaic/thermal system using various cooling methods. *Sustainable Energy Technologies and Assessments*. 51 (2022) 101844.
- [3] Q. Yu, X. Chen, H. Yang. Research progress on utilization of phase change materials in photovoltaic/thermal systems: A critical review. *Renewable and Sustainable Energy Reviews*. 149 (2021) 111313.
- [4] S.R. Maadi, M. Khatibi, E. Ebrahimnia-Bajestan, D. Wood. Coupled thermal-optical numerical modeling of PV/T module – Combining CFD approach and two-band radiation DO model. 198 (2019).
- [5] M. Li, D. Zhong, T. Ma, A. Kazemian, W. Gu. Photovoltaic thermal module and solar thermal collector connected in series: Energy and exergy analysis. *Energy Conversion and Management*. 206 (2020) 112479.
- [6] S.R. Abdallah, H. Saidani-Scott, O.E. Abdellatif. Performance analysis for hybrid PV/T system using low concentration MWCNT (water-based) nanofluid. *Solar Energy*. 181 (2019) 108-15.
- [7] M.R. Kalateh, A. Kianifar, M. Sardarabadi. Energy, exergy, and entropy generation analyses of a water-based photovoltaic thermal system, equipped with clockwise counter-clockwise twisted tapes: An indoor experimental study. *Applied Thermal Engineering*. 215 (2022) 118906.
- [8] G. Asefi, T. Ma, R. Wang. Parametric investigation of photovoltaic-thermal systems integrated with porous phase change material. *Applied Thermal Engineering*. 201 (2022) 117727.
- [9] M. Mortadi, A. El Fadar. Novel design of concentrating photovoltaic thermal collector– A comparative analysis with existing configurations. *Energy Conversion and Management*. 268 (2022) 116016.
- [10] A. Kazemian, M. Khatibi, T. Ma, J. Peng, Y. Hongxing. A thermal performance-enhancing strategy of photovoltaic thermal systems by applying surface area partially covered by solar cells. *Applied Energy*. 329 (2023) 120209.
- [11] A. Kazemian, B. Yaser, M. Khatibi, T. Ma. Performance prediction and optimization of a photovoltaic thermal system integrated with phase change material using response surface method. *Journal of Cleaner Production*. 290 (2021) 125748.
- [12] T. Ma, M. Li, A. Kazemian. Photovoltaic thermal module and solar thermal collector connected in series to produce electricity and high-grade heat simultaneously. *Applied Energy*. 261 (2020) 114380.
- [13] Z. Han, K. Liu, G. Li, X. Zhao, S. Shittu. Electrical and thermal performance comparison between PVT-ST and PV-ST systems. *Energy*. (2021) 121589.
- [14] A. Kazemian, A. Parcheforosh, A. Salari, T. Ma. Optimization of a novel photovoltaic thermal module in series with a solar collector using Taguchi based grey relational analysis. *Solar Energy*. 215 (2021) 492-507.
- [15] V. Suresh, S.M. Iqbal, K. Reddy, B. Pesala. 3-D numerical modelling and experimental investigation of coupled photovoltaic thermal and flat plate collector. *Solar Energy*. 224 (2021) 195-209.
- [16] C. Rajoria, S. Agrawal, G. Tiwari. Exergetic and enviroeconomic analysis of novel hybrid PVT array. *Solar Energy*. 88 (2013) 110-9.
- [17] S. Hassani, R. Saidur, S. Mekhilef, R.A. Taylor. Environmental and exergy benefit of nanofluid-based hybrid PV/T systems. *Energy Conversion and Management*. 123 (2016) 431-44.
- [18] A. Cetina-Quiñones, I. Polanco-Ortiz, P.M. Alonzo, J. Hernandez-Perez, A. Bassam. Innovative heat dissipation design incorporated into a solar photovoltaic thermal (PV/T) air collector: an optimization approach based on 9E analysis. *Thermal Science and Engineering Progress*. (2022) 101635.
- [19] S.R. Maadi, M. Khatibi, E. Ebrahimnia-Bajestan, D. Wood. A parametric study of a novel PV/T system model which includes the greenhouse effect. (2019).
- [20] M. Khatibi, M.M. Kowsari, B. Golparvar, H. Niazmand, A. Sharafian. A comparative study to critically assess the designing criteria for selecting an optimal adsorption heat exchanger in cooling applications. *Applied Thermal Engineering*. 215 (2022) 118960.
- [21] A. Kazemian, A. Salari, A. Hakkaki-Fard, T. Ma. Numerical investigation and parametric analysis of a photovoltaic thermal system

- integrated with phase change material. Applied Energy. 238 (2019) 734-46.
- [22] A. Kazemian, A. Salari, T. Ma, H. Lu. Application of hybrid nanofluids in a novel combined photovoltaic/thermal and solar collector system. Solar Energy. 239 (2022) 102-16.
- [23] W.C. Swinbank. Long-wave radiation from clear skies. Quarterly Journal of the Royal Meteorological Society. 89 (1963) 339-48.
- [24] A. Bejan, J. Kestin. Entropy generation through heat and fluid flow. (1983).
- [25] https://www.meteoblue.com/en/weather/historyclimate/climatemodelled/mashhad_iran_124665.
- [26] S. Entezari, A. Taheri, M. Khatibi, H. Niazmand. Acceleration of melting process of phase change material using an innovative triplex-tube helical-coil storage unit: Three-dimensional numerical study. Journal of Energy Storage. 39 (2021) 102603.
- [27] M. Khatibi, R. Nemati-Farouji, A. Taheri, A. Kazemian, T. Ma, H. Niazmand. Optimization and performance investigation of the solidification behavior of nano-enhanced phase change materials in triplex-tube and shell-and-tube energy storage units. Journal of Energy Storage. (2020) 102055.
- [28] <https://re.jrc.ec.europa.eu>.

التحليل السنوي للطاقة، والاكسيرجي، والبيئة (3E) لنظام مشترك من وحدة حرارية كهروضوئية ومجمع حراري شمسي

سمير ترف عزيز العارضي* محمد مقيمان**

**،* جامعة فردوسي في مشهد/ مشهد/ ايران

* البريد الإلكتروني: eng.sameer3@gmail.com

** البريد الإلكتروني: moghiman@um.ac.ir

الخلاصة

يتم تحليل الأداء السنوي لنظام هجين لنظام حراري ضوئي مستو وجامع حراري شمسي (PVT / ST) عددًا من منظور الطاقة، والطاقة الخارجية، والبيئة (تقليل ثاني أكسيد الكربون). يمكن لهذا النظام إنتاج طاقة كهربائية وحرارية في نفس الوقت وله طاقة حرارية وطاقة أعلى من الأنظمة الحرارية الكهروضوئية التقليدية. لهذا الغرض، تم تطوير نموذج رقمي عابر ثلاثي الأبعاد للتحقق من أداء النظام في أربع خطوات رئيسية: (1) التحقق في آثار معدل التدفق الكتلي لسائل العمل (20 إلى 50 كجم / ساعة) على سلوك درجة الحرارة؛ والديناميكا الحرارية لأداء النظام، (2) التحقق في آثار استخدام زجاج الغطاء على أجزاء مختلفة من النظام، (3) تقييم التحليل السنوي لاستهلاك الطاقة والطاقة للنظام في ظروف الطقس في مشهد، و (4) فحص الكربون. تقليل ثاني أكسيد باستخدام النظام المقترح تظهر النتائج أنه بالنسبة لنظام PVT / المزجج ST ((المزجج)، تؤدي زيادة معدل التدفق الكتلي لسائل العمل من 20 إلى 50 كجم / ساعة إلى تحسن بنسبة 22% و 1.5% في الطاقة الحرارية والكهربائية. على التوالي. ومع ذلك، تقل الطاقة الحرارية للنظام بنسبة 40.1%. بالإضافة إلى ذلك، ينتج نظام PVT / المزجج ST (طاقة حرارية أكثر بنسبة 86% ومعدل طاقة حرارية بنسبة 264% أكثر من نظام PVT / ST واستناداً إلى التحليل السنوي، تم إنتاج أعلى متوسط للطاقة الحرارية والكهربائية في شهر أغسطس بحوالي 338.3 و 24 وات على التوالي. تزداد كمية تقليل ثاني أكسيد الكربون مع ارتفاع معدلات تدفق الكتلة واستخدام زجاج الغطاء في كلا الجزأين. يمكن أن يقلل استخدام نظام PVT / (المزجج) من إنتاج ثاني أكسيد الكربون بمقدار 426.3 كجم سنويًا.